Communications

Discussion of "Microdistribution of Cerium in Steel"*

G. A. J. HACK

The authors Qiyong Han *et al.*, in their paper entitled "Microdistribution of Cerium in Steel", refer to the commercial oxide dispersion strengthened wrought material INCOLOY alloy MA 956 manufactured by Inco Alloys International. We believe that some clarification of the method of manufacture and properties of this alloy would be informative in the light of conclusions made in the paper.

1. INCOLOY alloy MA 956 is strengthened by a very finely distributed dispersion of yttrium oxide particles. These oxides comprise crystallites 20 to 40 nm in size which are mechanically alloyed into the matrix during manufacture. This alloy therefore is never melted at any stage during production between raw material powders and final wrought product. Moreover, apart from some fusion welds, the alloy would never be used following any type of melting operation as this would destroy the dispersoid structure and distribution, leading to total loss of the high temperature mechanical properties. Once melted, the alloy's unique feature of yttrium oxide dispersoids would be lost to slag formation and the material could no longer correctly be called INCOLOY alloy MA 956.

2. The chemical composition of the alloy investigated does not correspond to INCOLOY alloy MA 956, but appears to resemble a FeCrAl cast + wrought type of alloy. For example, the reported chromium and aluminum levels are much too high for INCOLOY alloy MA 956 and, if these represent melted material, would be even more anomalous. There is no reference to the most important alloying addition, yttrium oxide. The paper could give the impression that cerium is normally present in significant amounts in INCOLOY alloy MA 956. We would like to emphasize that no deliberate addition of cerium is made and none is likely to be present in significant amounts detectable by normal analytical means.

3. The only heat-treatments recommended for INCOLOY alloy MA 956 are at 1100 °C (stress relief, pre-oxidation of surface) and 1315 °C to 1350 °C (secondary recrystallization to coarse grain structure). It is not clear what was the intention of the authors' heat-treatment of 2 hours at 780 °C.

4. The authors refer to a paper by Golightly *et al.*[1] which describes the formation of yttrium enriched intergranular oxides acting as "pegs" for the alumina protective oxide on alloys prepared by melting with metallic yttrium as the alloying addition. The results of this work should not be confused with commercially available INCOLOY alloy MA 956 in which pre-existing ultra-fine particles of yttrium oxide are mechanically alloyed into the alloy matrix during manufacture. In the latter case, metallic yttrium is not available for subsequent oxide formation. A more closely related article describing alumina scale formation in INCOLOY alloy MA 956 prepared by mechanical alloying and not subsequently melted has been written by Ramanarayanan *et al.*[2] "Pegging" of the alumina protective oxide film on this alloy has been observed by Macdonald[3] following exposure for 500 hours at 1300 °C, but the pegs were identified as titanium-rich, probably carbonitrides, and not yttrium oxide enriched.

Detailed information including data sheets, articles, and technical papers is available on mechanically alloyed oxide dispersion strengthened superalloys such as INCOLOY* alloy MA 956, INCONEL* alloy MA 754, and INCONEL alloy MA 6000. These alloys, together with the mechanical alloying process, were developed by Inco, and, as alloy manufacturers, Inco Alloys International at Hereford, United Kingdom and Huntington, WV, we would be pleased to respond to further inquiries.

REFERENCES

1. F. A. Golightly, F. H. Stott, and G. C. Wood: *Oxidation of Metals*, 1976, vol. 10, pp. 163-87.
2. T. A. Ramanarayanan, M. Raghavan, and R. Petkovic-Luton: *Jour. Electrochem. Soc.*, 1981, vol. 131, no. 4, pp. 923-31.
3. D. M. Macdonald: Frontiers of High Temperature Materials Conf., 1981, London, Publ. IncoMAP.

*INCOLOY and INCONEL are trademarks of the INCO family of companies.

G. A. J. HACK is Industry Manager, Inco Alloys International, Holmer Road, Hereford HR4 9SL, United Kingdom.

Discussion submitted September 16, 1987.

Authors' Reply

QIYONG HAN, CHENGZHANG HUO, WEIZHEN ZHONG, and MING PENG

Mr. Hack's comments are right. The INCOLOY alloy MA 956 mentioned in our paper actually is an FeCrAl cast alloy. It is produced in China with the addition of Mischmetal. In the original manuscript, we called it FeCrAl alloy which is the Chinese alloy grade.

Nature of the γ and γ^* Phases in Austenitic Stainless Steels Cathodically Charged with Hydrogen

P. ROZENAK and D. ELIEZER

Hydrogen induced martensite phase transformation in austenite stainless steels has been extensively studied with respect to the relative stability of the austenitic phase. The

*QIYONG HAN, CHENGZHANG HUO, WEIZHEN ZHONG, and MING PENG: *Metall. Trans. A*, 1987, vol. 18A, pp. 499-507.

P. ROZENAK, formerly with the Materials Engineering Department, Ben-Gurion University of the Negev, Beer-Sheva, is with the Department of Materials Science, University of Illinois at Urbana-Champaign, 1304 West Green Street, Urbana, IL 61801. D. ELIEZER is Professor of Metallurgical Engineering, Department of Materials Engineering, Ben-Gurion University of the Negev, Beer-Sheva, Israel.

Manuscript submitted October 6, 1986.

effect of hydrogen on the γ-phase stability is that hydrogen decreases the γ-phase stability and may induce transformation of the γ-phase to α' and/or ε martensite.[1-9] H ingress occurred during electrolytic charging and egress after charging in the near surface layer of austenitic steel at room temperature.[10,11] In electrolytically charged stainless steels, X-ray diffraction lines from γ(fcc) and ε(hcp) phases were shifted (to larger 2θ values), while the lines from the α'(bcc) were found to remain constant during the aging process, indicating the limited ability of the α' phase to absorb hydrogen compared to the γ and ε phases.[12]

Mathias *et al.*[5] have proposed that the significant lattice expansion ($\gamma \rightarrow \gamma^*$) of the parent austenite occurs due to large amounts of hydrogen adsorption. In addition, it has been found that in austenitic steel (except AS 2 steel) hydrogenation also induces the formation of an expanded hexagonal phase (ε^*). Narita *et al.*[7] have suggested that the stainless steel H system appears to have a miscibility gap in which the γ phase, containing about 25 pct H, is in equilibrium with the γ^* phases, containing 55 pct H; *i.e.*, it is ferrogmagnetic with a Curie temperature below 273 K. An fcc hydride (H_γ) and an hcp hydride (H_ε) has been reported by Szummer and Janko[4] in cathodically charged stainless steel. These alloy hydride phases have the same crystal structures as hydrogen-free austenite and ε-martensite, respectively, but with about 5 pct larger lattice parameters. The appearance of two or more austenitic peaks after charging of stainless steels in the diffraction band and the relative shift of these peaks during aging were interpreted in different ways.

In the present study, we examined the effects of hydrogen on the γ phase in cathodically charged austenitic type 316 stainless steel. The γ^* transition and the kinetics of the transitions were investigated. An attempt was made to correlate the nature of these phases with hydrogen distribution in austenite.

The studies were carried out on AISI type 316 austenitic stainless steel. The steel was of commercial grade with the composition 16.8Cr, 13.2Ni, 2.7Mn, 0.41Si, 0.03C, 2.0Mo (wt pct). It was supplied in the form of 0.1 mm thick sheets. All the samples used in these experiments were solution annealed for 1 hour at 1100 °C. The grain size was ASTM 11 measured using the ASTM E-112 method.[13] Hydrogen charging was performed at room temperature in 1 N H_2SO_4 containing 0.25 g $\cdot$ l^{-1} of $NaAsO_2$ as a hydrogen recombination poison. A platinum counter electrode and a current density of 50 mA $\cdot$ cm^{-2} was used. A conventional Philips diffractometer equipped with a stepping motor and programmer was used for the X-ray diffraction study. The choice of X-ray wavelength is of special importance: in diffractions with reflection (Bragg-Brentano) geometry, only information from the thin surface layer of the flat sample is obtained. The intensity I_t of the rays scattered by the surface layer of thickness t is equal to:[14]

$$I_t/I_\infty = 1 - \exp/[-2\mu t/(\sin\theta)] \qquad [1]$$

where I_∞ is the intensity of the rays scattered by an infinitely thick sample, μ is the linear absorption coefficient of the material, and θ is the Bragg angle. The thickness, $t_{0.95}$, representing 95 pct of the total intensity of scattered rays, may be calculated from Eq. [1] for various diffraction peaks and radiations. For the 111 austenite peak for CuK_α, CoK_α, and CrK_α radiation, $t_{0.95}$ was found to be equal to 2.6, 6.2, and 8.7 μm, respectively. As has been reported elsewhere,[8] cracks produced by cathodic charging propagate inside the material to a depth of approximately 8 to 10 μm. It is essential to characterize this damage layer. The hydrogen content was determined in a LECO RH-1 hydrogen analyzer, which measures the mass of hydrogen released from the specimen during melting.

In electrolytic charging large amounts of hydrogen are driven into the specimen. The results of the hydrogen ingress study, presented as the amount of hydrogen remaining in the material *vs* time of charging of type 316 austenite stainless steel, are shown in Figure 1. Hydrogen with charging time gradually reached saturation in the steel, and after 48 hours of charging the hydrogen concentration was found to be about 335 ppm wt. X-ray diffraction patterns of 316 type taken after various times of charging and aging are shown in Figure 2 for shallow penetrating CuK_α radiation. ε-martensite was detected after 15 minutes of charging (Figure 2(a)). The γ and ε phase reflections exhibit significant broadening and they are shifted to smaller 2θ values, consistent with the presence of a large hydrogen concentration gradient. On diffractograms in the early stage of charging (5 minutes), splitting of $\gamma:\gamma^*$ peaks was observed. The γ^* has a larger lattice parameter than the γ phase. Continuous $\gamma \rightarrow \gamma^*$ contraction takes place as the charging times increase (Figures 2(a), (e)). After severe charging of 120 minutes this γ^*_{200} peak has an expanded d spacing, d = 1.888 Å, which is about 5.8 pct greater than that of the original austenite matrix. The intensity of diffraction lines reflected from the γ^* increased as the charging times increased. The ε(01.1) peak overlapped a weak α'(110) martensite peak immediately after cathodic charging. The amount of ε phase increased with increasing charg-

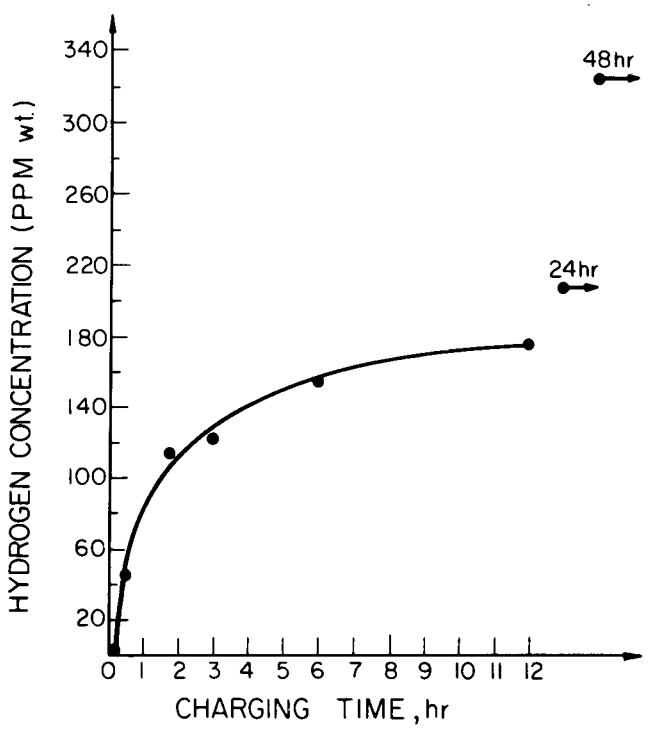

Fig. 1 — Hydrogen content *vs* charging time for 316 stainless steel at room temperature.

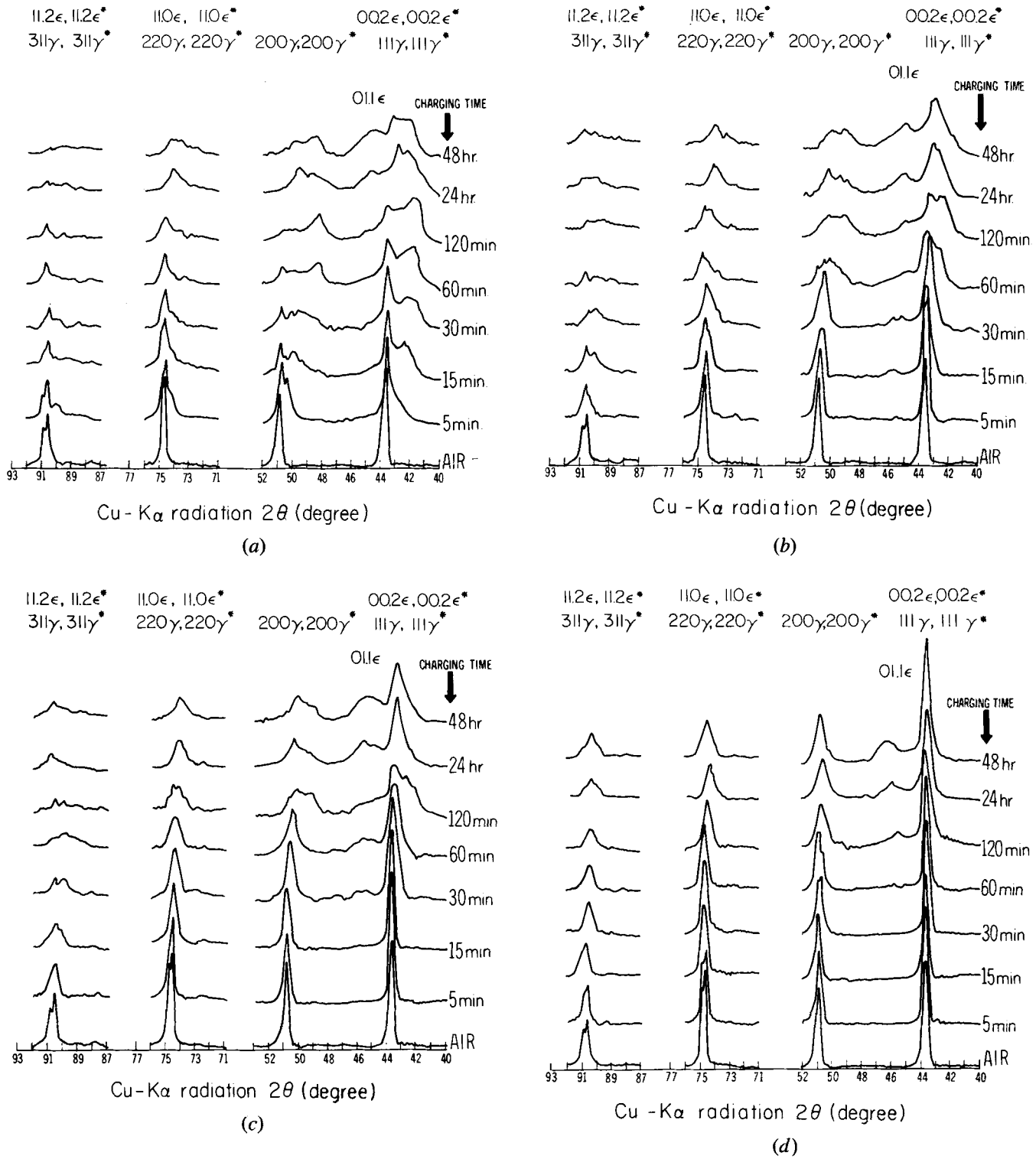

Fig. 2—X-ray diffraction patterns after indicating charging times (Cu-K_α radiation): (*a*) immediately after charging, (*b*) 30 min of aging, (*c*) 60 min of aging, (*d*) 4.5 h of aging, and (*e*) magnification of the region between 46-52, 2θ deg in (a).

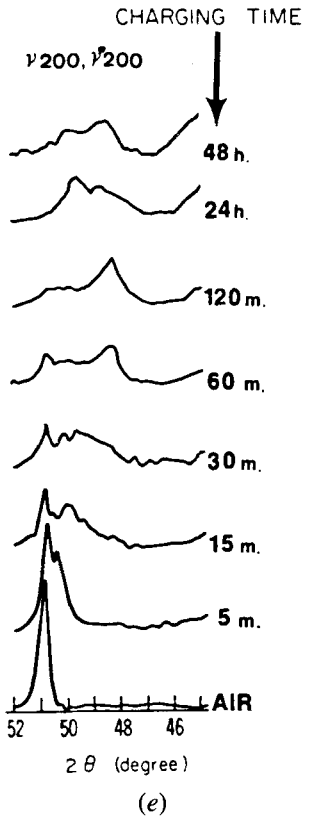

(e)

Fig. 2 Cont. — X-ray diffraction patterns after indicating charging times (Cu-K_α radiation): (*a*) immediately after charging, (*b*) 30 min of aging, (*c*) 60 min of aging, (*d*) 4.5 h of aging, and (*e*) magnification of the region between 46-52, 2θ deg in (a).

ing time and its 01.1 peak d spacing was approximately $d = 2.049$ Å after severe 48 hours charging. This lattice parameter is about 5.5 pct greater than those reported for the ε phase formed athermally or by plastic deformation.[8]

Aging after cathodic charging resulted in a number of significant structural changes. The γ^* phase reflections exhibit significant broadening and shifted continuously to higher 2θ values, indicating a decrease in lattice parameter. Due to overlap of γ^* and γ reflections the change in shape of γ^* peaks during aging was rather complicated (Figures 2(b), (c), and (d)). The split peaks shifted over to the regular position of the uncharged samples. This shift of the austenite, as well as the ε-martensite peaks, is accompanied by decreasing peak width. However, the peak broadening of ε-martensite decreases with aging time, but persists even after prolonged aging. The diffraction lines reflected from the hydrogenated layer are superimposed on those of the parent γ matrix, which are obviously increased if radiation of high CoK_α and CrK_α penetration power is utilized, suggesting that γ^* and ε phases were formed close to the specimen surface.[8,12] Diffractions, obtained when CrK_α high resolution radiation was used, showed that the γ^* appeared after 5 minutes charging, and 111, 200, 220, and 311 diffraction peaks from γ^* phase peaks appeared (Figure 3). The ε in this type of steel formed after 60 minutes of charging and a 01.1 diffraction peak from ε phase appeared. This information leads us to suggest that the hydrogen-induced phases probably appear in the sequence $\gamma \rightarrow \gamma^* \rightarrow \varepsilon$.

Changes in γ^*_{200} line positions and profile of γ_{200} in a 316 specimen after aging at 290 K temperature clearly show the

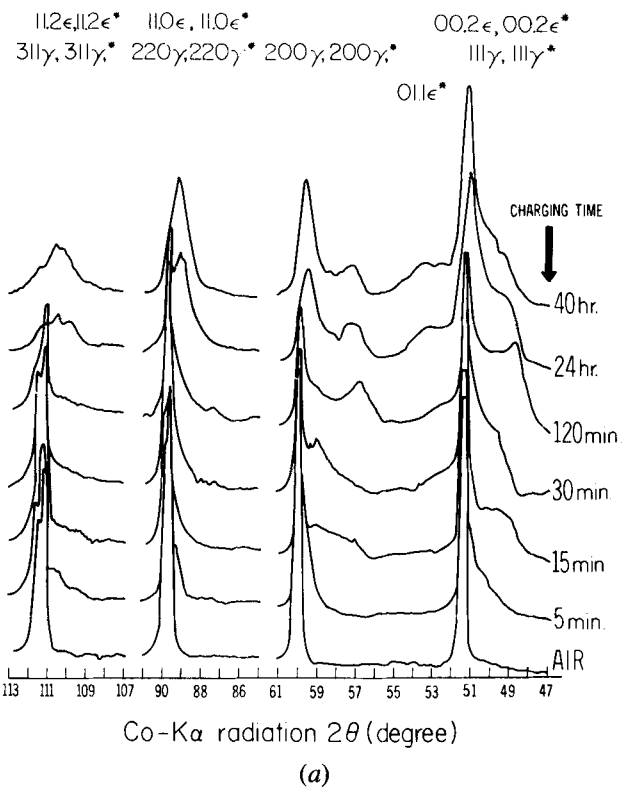

(a)

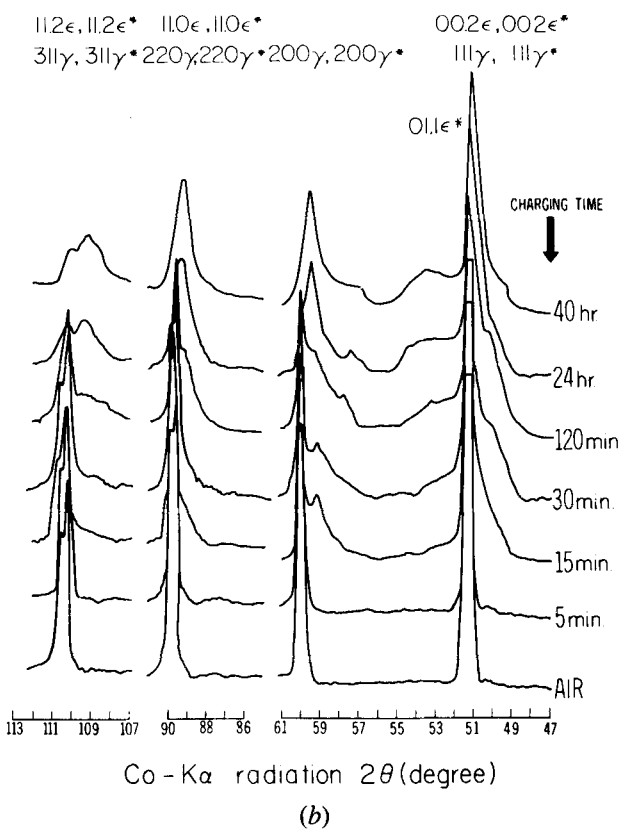

(b)

Fig. 3 — X-ray diffraction patterns after indicated charging times (Cr-K_α radiation).

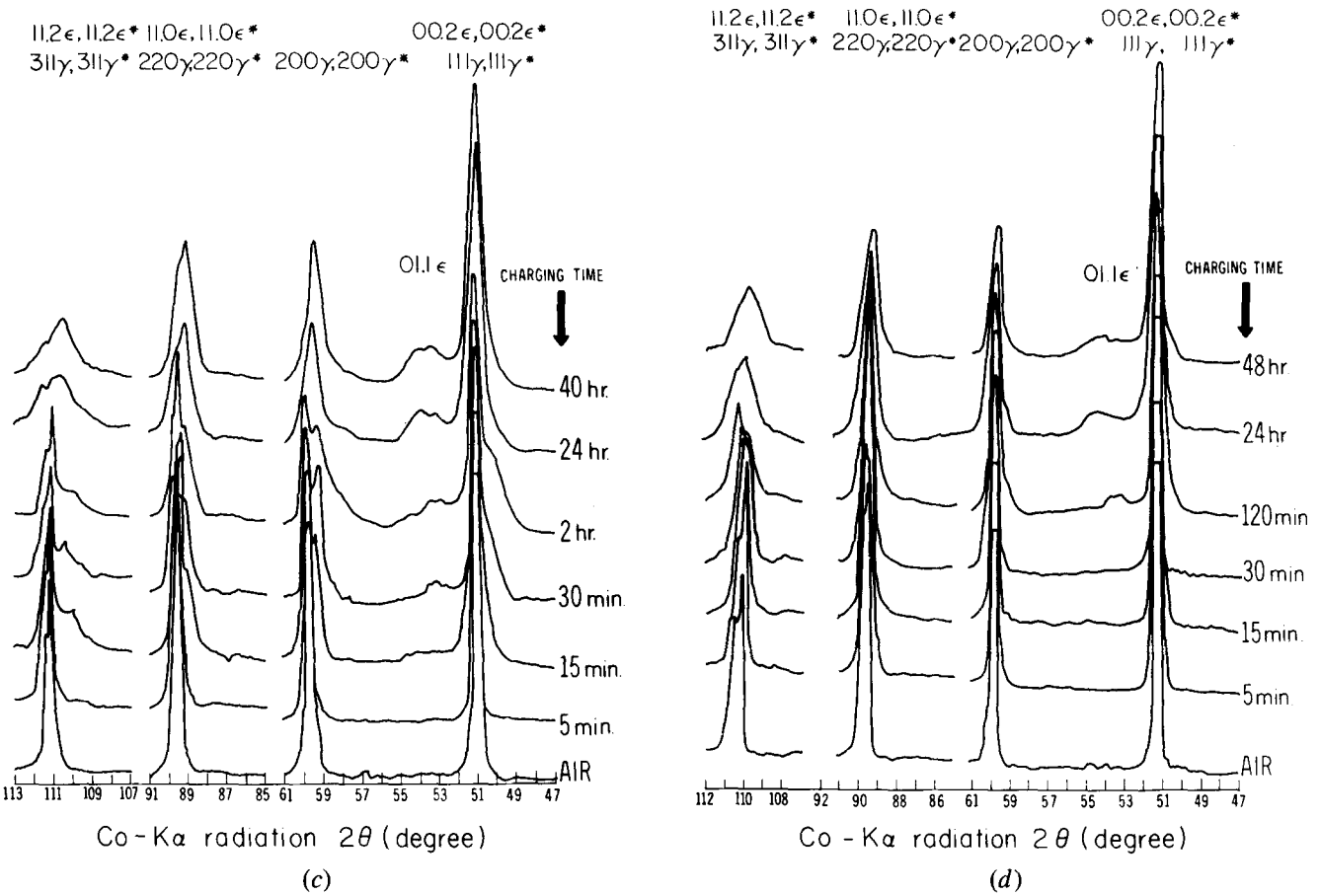

Fig. 3 Cont. — X-ray diffraction patterns after indicated charging times (Cr-K_α radiation).

typical continuous nature of lattice contraction of the γ^* during the aging (Figure 4). The intensity of the γ^* reflection increased and those of the γ phase did not change at short aging times. During the remaining aging, the γ^* lattice parameter decreased and the γ reflection intensities increased. Convolution of the diffraction profiles to γ_{200} and γ^*_{200} after aging (originally 1 hour cathodically charged) are shown in Figure 5. Profile A obtained from a diffraction line reflected from the nonhydrogenated austenite and profiles B and C were obtained from γ^* that caused by hydrogen distribution in metallic layers after cathodic charging at room temperature. The typical continuous nature of lattice contraction (shift of profiles B and C to larger 2θ values, consistent as the hydrogen diffused out of the specimen) of the γ^* during aging was confirmed experimentally in the present study. Thus the data lead us to suggest, in the hydrogen charged steels, continuous transformation of γ^* to γ as the hydrogen outgasses from the specimen.

The present observations of the phase transformations induced by cathodic charging of stainless steels, suggest that the hydrogen concentration in the surface region must play a significant role. At the surface the hydrogen fugacity, which depends on the detailed surface chemistry, has been estimated to be at least 10^8 atmospheres.[15] The high fugacity during cathodic charging will induce a high near surface concentration of hydrogen, and the relatively low diffusivity of hydrogen in austenite ($D_H \sim 8 \times 10^{-16}$ m^2/sec at 300 K[7] will cause a high concentration gradient over shallow depths into the specimen. Atrens *et al.*[10] have calculated concentration profiles resulting from hydrogen charging of austenite and have shown that during the aging after charging (two hours at 298 K) the hydrogen concentration falls by a factor of 10 within the first 5 μm of the surface. Thereafter, during aging, the hydrogen concentration is zero at the surface, and increases to a maximum and decreases again with increasing depth. Farrell and Lewis[11] made direct measurements of deuterium profiles and have shown that the concentration of hydrogen (deuterium) is in the near surface layers of 310 austenitic steel following room temperature cathodic charging. Aging curves following an ingress time of 600 seconds showed that the front of the profile continues spreading inward but the deuterium in the immediate surface layers escape to the atmosphere; the maximum concentration declines and moves inward. During the aging process it is expected that hydrogen loss will occur primarily through the external surface. The hydrogen concentration during aging is quickly reduced to low values at the surface and reaches a peak just below the surface and decreases at greater depths.

The peak broadening (Figures 2 through 5) was the result of the formation of a nonuniform solid solution of hydrogen in austenite. Since both hydrogen penetration during charging and hydrogen release during aging are diffusion controlled, large hydrogen concentration gradients in the thin surface layer of depths comparable with the depth of X-ray penetration are expected. Actually, the hydrogen concentration is nonuniform within a single grain and this nonuniform concentration of hydrogen results in nonuniform

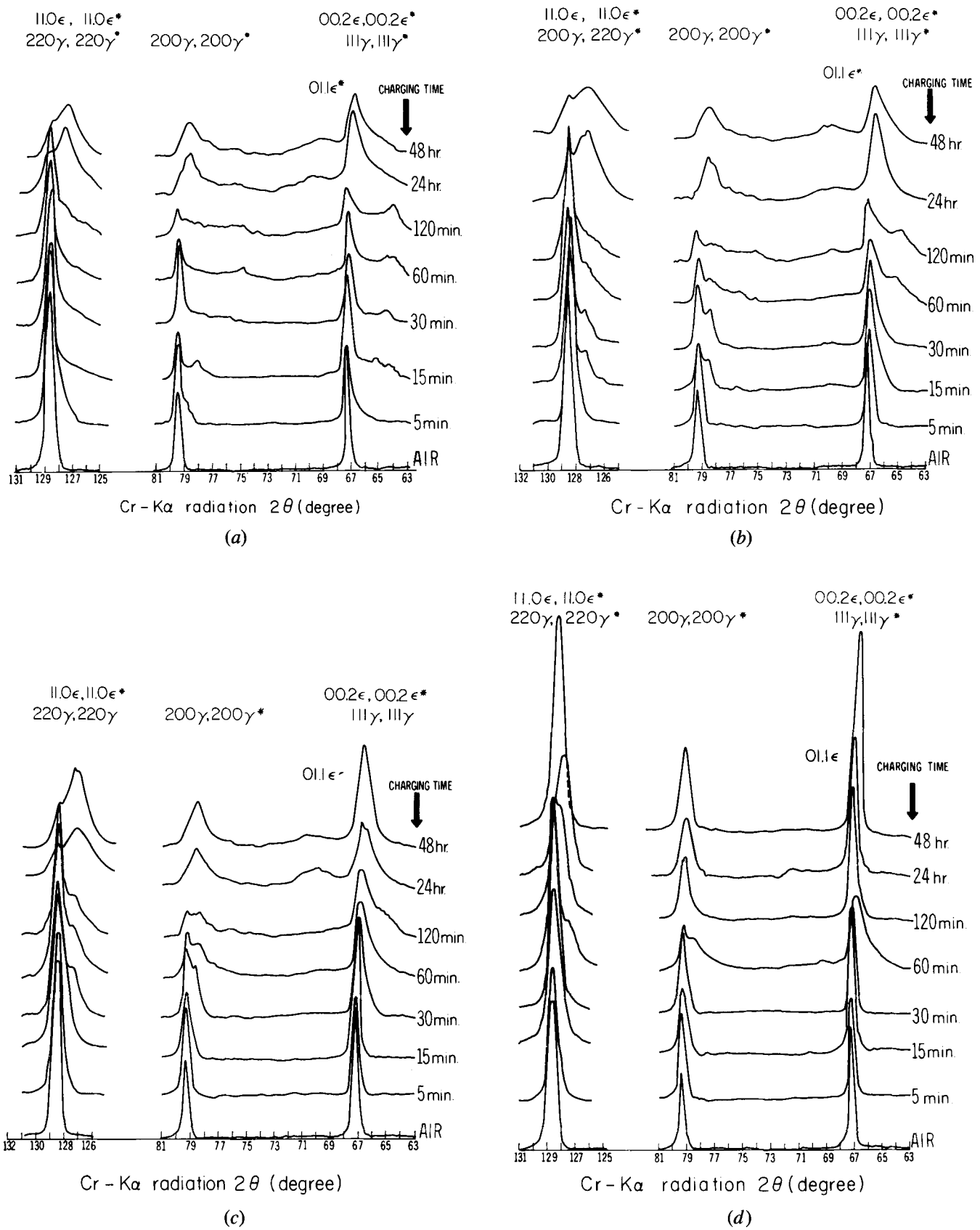

Fig. 4—Behavior of the expanded γ^*_{200} peak in the vicinity of the γ_{200} peak after aging at 298 K (originally 1 h cathodically charged) for the times indicated. (*a*) Cu-K_α radiation, (*b*) Co-K_α radiation, and (*c*) Cr-K_α radiation.

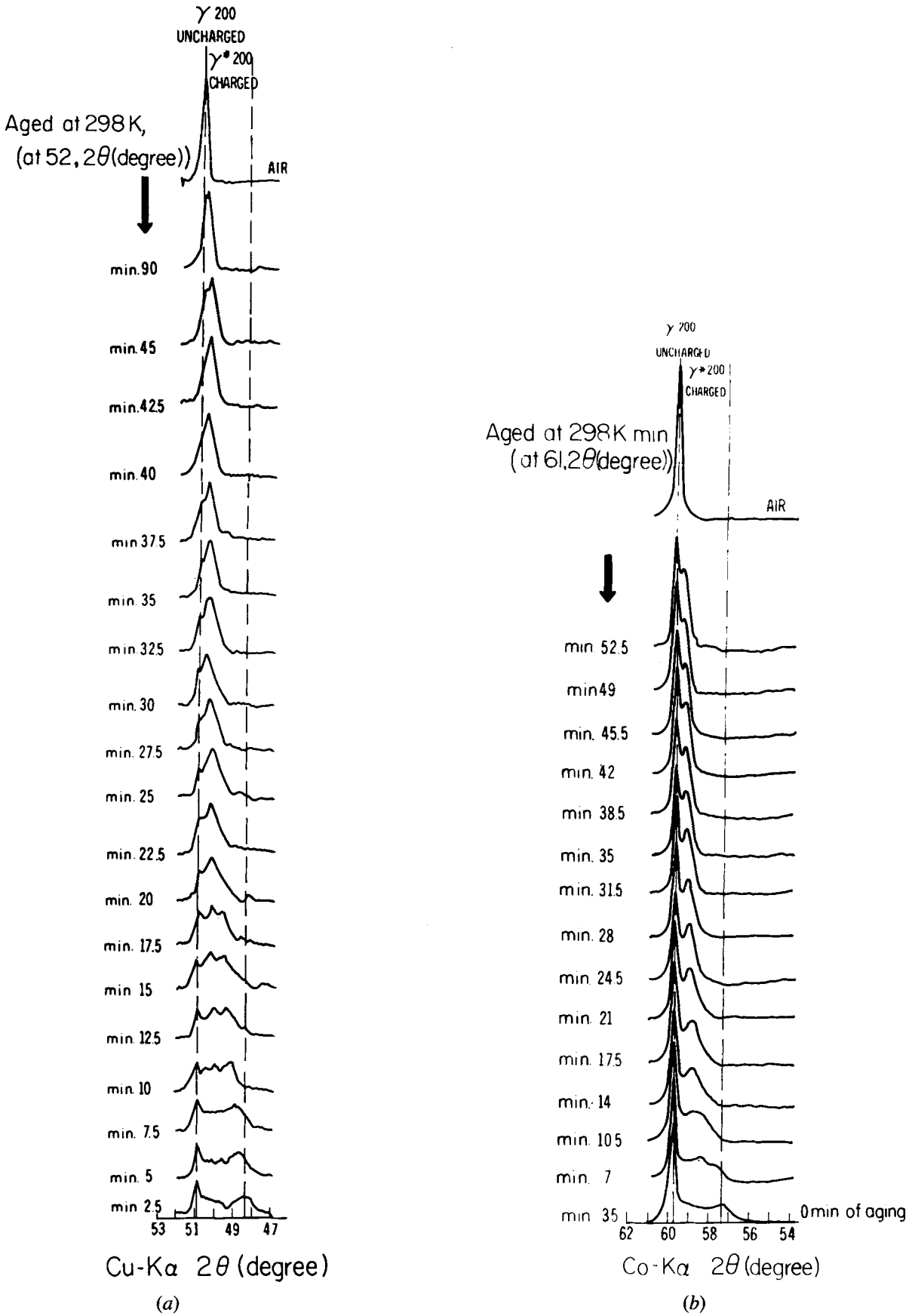

Fig. 5 — Convolution of the diffraction profiles of γ_{200} and γ^*_{200} after aging at 298 K (originally 1 h cathodically charged) for the times indicated.

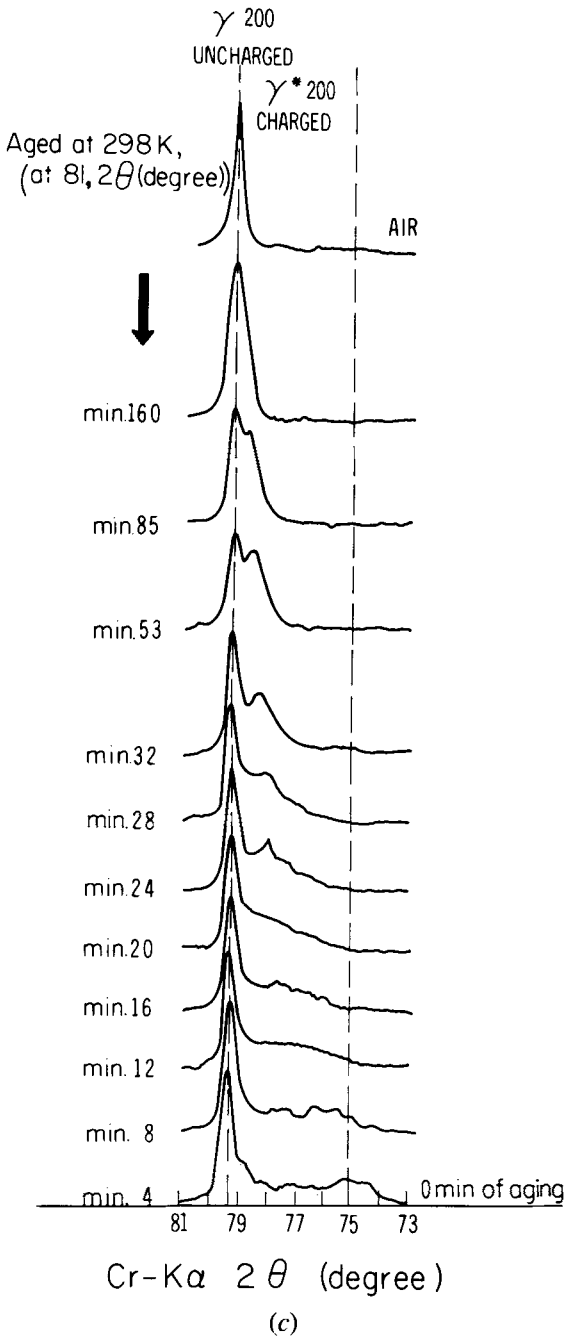

(c)

Fig. 5 Cont. — Convolution of the diffraction profiles of γ_{200} and γ^*_{200} after aging at 298 K (originally 1 h cathodically charged) for the times indicated.

expansion, which in turn leads to the development of the internal stresses.[8,12] Stress relaxation should consequently occur; evidence of such relaxation is obtained from the crack formation during the aging.[1,16–20]

Generally, hydrogen might be influential due to the alloying effects, to the alteration of transformation temperatures (M_s or M_d), or to affecting the stacking fault energy (SFE). Internal stresses or strains which accompany the absorption of the supersaturated hydrogen might provide a significant driving force for austenite decomposition. In particular, changes occurring in the M_s-M_d temperature range should be considered, since metastable austenite can be activated by an external or internal stress field. Hydrogen decreases the γ-phase stability and induces transformations of the γ-phase to ε and α'-martensites. Following the termination of hydrogen charging, continuous $\gamma \rightarrow \gamma^*$ expansion takes place and during the aging continuous $\gamma^* \rightarrow \gamma$ contraction takes place, with hydrogen release, as has been confirmed experimentally.

The appearance of two or more peaks in the diffraction band and the relative shift of these peaks during aging were interpreted as evidence for the existence of two different austenitic phases with low and high hydrogen concentrations and a miscibility gap between them.[4,7] Thus, the nature of the diffraction band obtained is a result of the inhomogeneous continuous distribution of the hydrogen in the surface of cathodically charged and aged specimens.

In cathodically charged austenitic type 316 steel the appearance of γ^* is a result of the particular hydrogen distribution in the sample after the charging and during the outgassing.

REFERENCES

1. M. Holzworth and M. Louthan, Jr.: *Corrosion*, 1968, vol. 24, pp. 110-24.
2. P. Maulik and J. Burke: *Scripta Metall.*, 1975, vol. 9, pp. 17-22.
3. J. M. Rigsbee: *Metallography*, 1978, vol. 11, pp. 493-98.
4. A. Szummer and A. Janko: *Corrosion*, 1979, vol. 35, pp. 461-54.
5. H. Mathias, Y. Katz, and S. Nadiv: *Metal Science*, 1978, vol. 12, pp. 129-37.
6. N. Narita and H. Birnbaum: *Scripta Metall.*, 1980, vol. 14, pp. 1355-58.
7. N. Narita, C. J. Altstetter, and H. K. Birnbaum: *Metall. Trans. A*, 1982, vol. 13A, pp. 1355-65.
8. P. Rozenak, L. Zevin, and D. Eliezer: *J. Mat. Sci.*, 1984, vol. 19, pp. 567-73.
9. J. Chene: *Current Solutions to Hydrogen Problems in Steels*, C. G. Interrante and G. M. Pressouyre, eds., ASM, Metals Park, OH, 1982, pp. 263-71.
10. A. Atrens, J. Bellina, N. Fiore, and R. Coyle: *The Metal Science of Stainless Steel*, E. Collings and H. King, eds., AIME, New York, NY, 1979, pp. 54-69.
11. K. Farrell and M. B. Lewis: *Scripta Metall.*, 1981, vol. 15, pp. 661-64.
12. P. Rozenak and D. Eliezer: *Acta Metall.*, 1987, vol. 35, no. 9, pp. 2329-40.
13. ASTM Standard E-112, 1977.
14. H. P. Klug and L. E. Alexander: *X-ray Diffraction*, John Wiley, New York, NY, 1974, p. 360.
15. A. Kumnick and H. Johnson: *Metall. Trans. A*, 1975, vol. 6A, pp. 1087-91.
16. H. Okada, Y. Hosoi, and S. Abe: *Corrosion*, 1970, vol. 26, pp. 83-186.
17. C. L. Briant: *Metall. Trans. A*, 1979, vol. 10A, pp. 181-89.
18. D. Eliezer, D. Chakrapani, C. Altstetter, and E. N. Pugh: *Metall. Trans. A*, 1979, vol. 10A, pp. 935-41.
19. R. Liu, N. Narita, C. Altstetter, H. Birnbaum, and E. N. Pugh: *Metall. Trans. A*, 1980, vol. 11A, pp. 1963-74.
20. R. C. Wasileuski and M. R. Louthan, Jr.: *Microstructural Science*, 1985, vol. 12, pp. 406-19.